Post-Combustion Emissions Control for Aero-Gas Turbine Engines

by

Prakash Prashanth

B.Eng., Mechanical Engineering
National University of Singapore (2016)

Submitted to the Department of Aeronautics and Astronautics
in partial fulfillment of the requirements for the degree of

Master of Science in Aeronautics and Astronautics

at the

MASSACHUSETTS INSTITUTE OF TECHNOLOGY

June 2018

Signature redacted

Author .....
Department of Aeronautics and Astronautics
May 21, 2018

Signature redacted

Certified by .....
Steven R. H. Barrett
Associate Professor of Aeronautics and Astronautics
Thesis Supervisor

Signature redacted

Accepted by .....
Hamsa Balakrishnan
Associate Professor of Aeronautics and Astronautics
Chair, Graduate Program Committee

Post-Combustion Emissions Control for Aero-Gas Turbine Engines

by

Prakash Prashanth

Submitted to the Department of Aeronautics and Astronautics
on May 21, 2018, in partial fulfillment of the
requirements for the degree of
Master of Science in Aeronautics and Astronautics

Abstract

Aviation NO_x emissions have an impact on air quality and climate change, where the latter is magnified due to the higher sensitivity of the upper troposphere and lower stratosphere. In the aviation industry, efforts to increase the efficiency of propulsion systems are giving rise to higher overall pressure ratios which results in higher NO_x emissions due to increased combustion temperatures. This thesis identifies that the trend towards smaller engine cores (gas generators) that are power dense and contribute little to the thrust output presents new opportunities for emissions control that were previously unthinkable when the core exhaust stream contributed significant thrust.

This thesis proposes and assesses selective catalytic reduction (SCR), which is a post-combustion emissions control method used in ground-based sources such as power generation and heavy-duty diesel engines, for use in aero-gas turbines. The SCR system increases aircraft weight and introduces a pressure drop in the core stream. The effects of these are evaluated using representative engine cycle models provided by a major aero-gas turbine manufacturer.

This thesis finds that employing an ammonia-based SCR can achieve close to 95% reduction in NO_x emissions for $\sim$0.4% increase in block fuel burn. The large size of the catalyst needs to be housed in the body of the aircraft and hence would be suitable for future designs where the engine core is also within the fuselage, such as would be possible with turbo-electric or hybrid-electric designs. The performance of the post-combustion emissions control is shown to improve for smaller core engines in new aircraft in the NASA N+3 time-line (2030-2035), suggesting the potential to further decrease the cost of the $\sim$95% NO_x reduction to below $\sim$0.4% fuel burn.

Using a global chemistry and transport model (GEOS-Chem) this thesis estimates that using ultra-low sulfur ($<$15 ppm fuel sulfur content) in tandem with post-combustion emissions control results in a $\sim$92% reduction in annual average pop-

ulation exposure to $PM_{2.5}$ and a ~95% reduction in population exposure to ozone. This averts approximately 93% of the air pollution impact of aviation.

Thesis Supervisor: Steven R. H. Barrett
Title: Associate Professor of Aeronautics and Astronautics

Acknowledgments

Firstly, I would like to thank Prof. Steven Barrett, for giving me the opportunity to come to MIT and join this wonderful lab that is LAE. Steven's perspective on problems and enthusiasm to tackle challenges with bold ideas has truly been an inspiration. I would like to thank Dr. Raymond Speth for guiding me thorough numerous technical aspects throughout this thesis. Ray's probing questions and attention to detail have helped me grow as a researcher. Dr. Jayant Sabnis's, experience, insight and fascinating anecdotes have always captivated and inspired me. I owe many thanks to Dr. Sebastian Eastham who has been the most patient person, guiding me as I learnt how to use new tools and putting up with the times I almost broke the server.

I cannot imagine the last two years without my labmates - Ines, Drew, Thibaud, Carla and Haofeng. Thank you for the discussions that have ranged from outright stupid to deep and profound. I look forward to the rest of my grad life with you guys. Ines, thank you for literally being by my side since our first semester, for our morning coffee runs, for ensuring we go to Muddy Fridays and reminding me to chill. Drew, thank you for being the most cheerful, animated one amongst us, for taking us to cool events, making the amazing LAE events calendar, and adjusting to SI units (real units) while talking to the rest of us. Thibaud, you are probably one of the smartest guys I know, thank you for being patient as I learnt how to use the server, the terminal and vim. Thank you for being my buddy taking all the "cool" fluid dynamics courses. Carla, thank you for all the advice you have given me so far and for helping me establish the right terminology when it comes to spatial location for lunch. I want to thank you and Paul for also helping me think thorough my choices while I was deciding to stay on for a PhD. Haofeng, thank you for being the one who challenges assumptions, shares random ideas from various books and for the late night conversations in lab.

To my flatmates, Suhas and Dheeraj, thank you for teaching me so much about

math, philosophy, politics and other random things. Thank you for both doing stupid things with me and for talking me out of doing stupid things.

Lastly I want to thank my family – Atthai and Chitti, thank you for being the best aunts ever. Atthai, thank you for being so encouraging, for reminding me of my successes and always exaggerating everything I do to make them sound like stellar achievements! Chitti and Chittappa thank you for all the love and support, from getting me so many books and Lego toys as a kid to dropping me off at MIT two years ago. You have been a great influence on my life.

Finally to the people to whom I owe it all – Amma, Appa and Shashank. Thank you for believing in me even when I sometimes did not. Amma, thank you for being the strongest person I know, for the unconditional love and always encouraging me, no matter what I was doing. Appa, thank you for teaching me so many things, always challenging me, and inspiring me with simple yet beautiful ideas. Shanky, you are the reason the last 20 years of my life have been so much better than the first 5. Thank you for always being there for me. Your humor, creativity, problem solving skills and eye for design never fail to inspire me. I hope to make you all proud.

Contents

List of Figures

List of Tables

Chapter 1

Introduction

Emissions of oxides of nitrogen (NO_x) adversely impact air quality and human health [8, 20]. NO_x is a precursor of fine particulate matter with an aerodynamic diameter of less than 2.5 μm ($PM_{2.5}$) and ozone (O_3). NO_x emitted at cruise altitude produces O_3 that upon reaching the surface alters the background chemistry to increase the concentrations of ground level $PM_{2.5}$. $PM_{2.5}$ and ozone cause asthma, cardiovascular and respiratory diseases [8, 20], and increase risk of early death. NO_x emissions from the global aviation industry have been estimated to cause ~16000 premature mortalities annually worldwide [11]. With the current growth rate of the aviation industry at an average of 5% per year [6], the absolute and relative contribution of aviation NO_x emissions to air pollution is also set to increase over the coming decades. Furthermore, local air quality degradation near airports inhibits airport expansion. NO_x also has an adverse impact on the climate, causing a short-term warming effect on the order of aviation CO_2, with a long-term cooling effect due to methane consumption [9].

In the commercial aviation sector, gas turbines have been the primary choice of power plant since the early 1950s [7] due to their high power density. The thermodynamic efficiency of the gas turbine increases with higher overall pressure ratio (OPR). The higher OPR leads to increased thermal NO_x production as the compressor exit temperature increases with the OPR [24]. Various combustor design strategies such as RQL (rich-quench-lean) combustion chambers have provided some control over the

NO_x emissions but are limited in the extent of NO_x reduction. The premise of the following work is that post-combustion treatment of the NO_x emissions can expand the design space for new engine architectures and enable further sustainable growth of the aviation sector by virtually eliminating aviation NO_x emissions while ensuring compliance with air quality and climate related emission standards.

1.1 Post-combustion emissions control in other industries

Heavy-duty diesel engines and the power generation industry routinely use post-combustion control to reduce their emissions. Comparing an aircraft engine and an aero-derivative engine used for power generation, NO_x emissions from aero-derivative engines are about an order of magnitude lower than the original engines used in an aircraft [25]. This is in part due to the choice of a gaseous fuel – natural gas used in power generators reduces the flame temperature [25] and hence NO_x emissions. A liquid fuel will result in local regions of stoichiometric conditions as the fuel droplets evaporate [23], resulting in local high temperature pockets, that increase NO_x formation. However, the bulk of the emission reduction (over 90%) comes from post-combustion emissions control that is primarily in the form of selective catalytic reduction (SCR).

The success of post-combustion emissions control in the road transportation sector is exemplified by the US EPA certification data from the diesel engine industry. Prior to 1991, diesel engines in automobiles required no aftertreatment and the average engine out NO_x emissions were 4.6 g/kWh. By 2013 emission regulations forced all on-road engines to use after treatment measures to control emissions. The average NO_x out from a diesel engine with SCR was brought down to 0.27 g/kWh [18]. This corresponds to approximately 94% reduction in NO_x emissions over two decades. Modern engines using SCR reduce NO_x emissions by 95% to 98% [19].

1.2 Selective catalytic reduction (SCR)

SCR converts oxides of nitrogen (NO and NO_2) to N_2 and H_2O in presence of a catalyst using a reducing agent, which is typically ammonia based. It is one of the most effective methods available to control NO_x emissions [21]. The following section describes the reaction pathways and characteristics of the catalysts used.

1.2.1 SCR pathway

The two main reactions for the reduction of NO_x are [21, 38]:

$$4NO + 4NH_3 + O_2 \longrightarrow 4N_2 + 6H_2O$$

$$NO + NO_2 + 2NH_3 \longrightarrow 2N_2 + 3H_2O$$

Typical diesel engine (and gas turbine) exhaust NO_x mainly consists of NO (>90%) [21], hence the first of the two reactions is the primary reaction for $DeNO_x$ (conversion of NO_x to N_2 and H_2O) with ammonia. In some applications, an oxidizing catalyst is used upstream of the SCR catalyst to convert NO to NO_2 since the second reaction with equimolar concentration of NO and NO_2 is faster than the first reaction. This work only considers the first reaction as gas turbine emissions are also predominantly NO (approximately 95%) [33], except at very low thrust conditions [36] – which are, however, relevant for approach and taxi operations.

1.2.2 SCR catalysts and substrates

Different catalytic materials are used in SCR depending on the application. Low temperature SCR uses platinum group metals (PGM), while higher temperature applications use vanadium and titanium oxides. Recent work has been focused on zeolite based catalysts, which have a broader operating temperature range, high conversion efficiency and are cheaper than PGM catalysts [31, 29]. The arrangement of interest in this work are cellular monolithic catalysts. Monolithic catalysts are extruded

corderites with a catalytic wash-coat, the straight channels of these monoliths reduce the pressure drop associated with the flow through the channels. Reference [40] provides relevant properties of the monolithic catalyst.

1.2.3 Reducing agents

The reducing agents used for the SCR reactions are ammonia based solutions [19]. A urea based solution (marketed as AdBlue or Diesel Engine Fluid (DEF)) is used by mobile SCR systems on road. Urea solutions are used (instead of pure ammonia) for on road applications due to safety concerns over handling pressurized pure anhydrous liquid ammonia. During the SCR process the ammonia based reducing agent is injected into the exhaust stream which then evaporates and mixes with the gas upstream of the catalyst. Properties of the reducing agents are given in Table 1.1.

Table 1.1: Properties of reducing agents [14]. AdBlue is a commercially used 32.5% urea solution for diesel engines. X_{m,NH_3} represents the moles of NH_3 contained in one kilogram of the reductant [14]. The fuel-specific reductant consumption (FSRC) is calculated for an assumed cruise EI(NO_x) of 14 g/kg fuel. $\dot{m}_{\text{Red}}$ and $\dot{m}_f$ are the reductant mass flow rate and fuel mass flow rate, respectively.

Reducing agent	**Molecular formula**	**Density**	$\mathbf{X_{m,NH_3}}$	**(FSRC)** $\frac{\dot{m}_{\text{Red}}}{\dot{m}_f}$
-	-	(kg/m^3)	(mol NH_3/kg reductant)	(g reductant/ kg fuel)
AdBlue	$(NH_2)_2CO + H_2O$	1086	10.8	28.1
Solid urea	$(NH_2)_2CO$	1330	33.3	9.14
Anhydrous liq ammonia	NH_3	610	58.7	5.18

1.3 Challenges to implementing SCR on aircraft gas turbine engines

Compared with road vehicles, aircraft fuel consumption is more sensitive to the mass of the vehicle. The mass flow rates through the core of a gas turbine engine used to power an A320 size aircraft during curise is on the order of 25-30 kg/s. This is the mass flow that needs to be treated by the catalyst. For comparison, a heavy duty diesel engine has a mass flow rate on the order of 1 kg/s. The ideal operating

temperature range for ion-exchanged zeolite SCR catalysts is approximately 550-650 K [17]. This temperature range generally occurs after the low pressure turbine (LPT) for the engine class under consideration. Installing a catalyst monolith downstream of the LPT will cause a pressure drop downstream of the turbine, thus reducing the work that it can extract. In order to maintain the required thrust, the fuel flow to the engine needs to be increased from the baseline case (with no catalyst), thus increasing the thrust specific fuel consumption (SFC). In the past, these weight and SFC concerns had discouraged any investigation into the use of SCR in aircraft [25].

However, with new architectures like the geared turbofan and the development of small core engines [26], the core size (defined as the corrected mass flow rate at the exit of the high pressure compressor) is smaller than current engines. The smaller, power dense core implies that a smaller mass of exhaust gas needs to be treated for a fixed engine thrust, which mitigates the impact of a pressure drop in the core exhaust stream. Furthermore, these cores contribute little to the overall engine thrust. For example, approximately 8.0% of the gross thrust in a geared turbofan comes from the core exhaust and we estimate that for a small core engine as described by Lord et al. [26] the core flow will contribute 3.6% of the gross thrust. This presents a new opportunity to apply a SCR based system to reduce the NO_x emissions from the engine. This work quantifies the additional fuel burn (which is proportional to CO_2 emissions) incurred for a certain level of NO_x reduction relative to a baseline design. We note that future designs are still likely to result in absolute reductions in fuel burn and CO_2.

In the following sections we evaluate an SCR system installed downstream of the LPT which treats the exhaust in the core flow of the engine. The reducing agent (pure anhydrous liquid ammonia) is sprayed at a suitable point (described in the section 3.9) upstream of the catalyst which gives sufficient time to mix with the exhaust before flowing through the catalyst.

Chapter 2

Methods

This section outlines the approach taken to evaluate the implementation of ammonia-based SCR of NO_x on aircraft gas turbine engines. After sizing the catalyst, we quantify the pressure drop through the monolith and use an engine model to calculate the increase in SFC. We then calculate the increase in fuel burn from the baseline case due to the additional weight of the reducing agent and the catalyst and the increased SFC due to the pressure loss in the catalyst. Using global atmospheric modeling tools and the calculated reduction in NO_x we then estimate the effect this has on ground level $PM_{2.5}$ and O_3 concentrations.

2.1 Mass transfer in monolithic catalyst and SCR model

The SCR process consists of bulk mass transfer, diffusion through the pores of the catalyst wash coat, followed by chemical reaction at the catalytic site. Each of these processes is temperature dependent — as the temperature increases, the chemical reaction rate increases exponentially [28] while the diffusion coefficients of the gas increases approximately with $T^{\frac{3}{2}}$ [28]. Therefore, at sufficiently high temperatures (T>500 K), the bulk diffusion or mass transfer becomes the limiting process [38]. This operating regime is referred to as the mass transfer-limited regime.

In this section we describe a lumped parameter model of the monolithic reactor. Tronconi [39] showed the adequacy of lumped parameter models for simulating SCR reactors, finding an average percentage error between experiments and the lumped one-dimensional model of 1.3%. In this model, average values of velocity and non-dimensional species concentration over the channel cross-section are used. The non-dimensional NO concentration is represented by $\Gamma = [NO]/[NO]_0$, where [NO] is the local concentration of NO and $[NO]_0$ is the concentration of NO at the inlet to the catalyst channel.

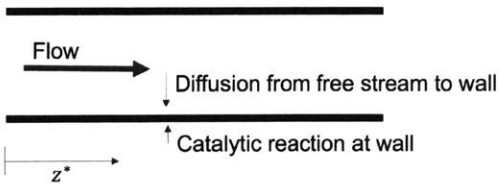

Figure 2-1: Illustration of flow through a channel. The variable z^* represents the non-dimensional co-ordinate in the direction of flow, $z^* = (zD_{NO})/(ud^2)$, where D_{NO} is the diffusivity of NO, d is the hydraulic diameter of the channel, z is the axial distance and u is the local flow velocity.

Considering Fig 2-1, we apply a mass balance for a reactant species, NO_x in the bulk phase (free stream) and another mass balance at the wall.
In the bulk phase,

$$\frac{d\Gamma}{dz^*} = -4\mathrm{Sh}(z^*)(\Gamma - \Gamma_{\mathrm{wall}}), \tag{2.1}$$

and at the wall,

$$\mathrm{Sh}(z^*)(\Gamma - \Gamma_{\mathrm{wall}}) = \mathrm{Da}\Gamma_{\mathrm{wall}}, \tag{2.2}$$

where $\mathrm{Sh}(z^*)$ is the local Sherwood number and Da is the Damköhler number. z^* is the non-dimensional axial distance defined as $z^* = (zD_{NO})/(ud^2)$. The Sherwood number represents the ratio of convective mass transfer to diffusive mass transfer, while the Damköhler number, in this context, represents the ratio of rate of chemical reaction of a species to the mass transfer rate, i.e. the ratio of the rate at which a species reacts at the catalyst wall to the rate at which the species is transported to the wall. Based on the work done by Tronconi [39] we can express the efficiency of

the catalyst in converting the NO_x in the exhaust as a fraction as

$$\mathrm{DeNO_x} = 1 - \Gamma = \exp\left(-4\int_0^{z^*} \frac{\mathrm{DaSh}}{\mathrm{Da}+\mathrm{Sh}}\mathrm{d}z^*\right). \tag{2.3}$$

2.2 Pressure drop in monolithic catalysts

Installing an SCR catalyst downstream of the turbines introduces a pressure drop associated with the flow through a monolith. We estimate the pressure drop the fluid experiences with [30]

$$\Delta P = 4f\frac{l}{d} \times \frac{1}{2}\rho v^2,$$

where f is the Fanning friction factor, l is the length of the channel, d is the hydraulic diameter of the channel and $\frac{1}{2}\rho v^2$ is the dynamic pressure of the flow. If the flow regime is laminar (as is almost always the case [30]) then the friction factor $f = \frac{14.23}{\mathrm{Re}}$, where $\mathrm{Re} = \frac{\rho v d}{\mu}$ (for square channels), ρ is the density, μ is the dynamic viscosity, and v is the local flow velocity of the exhaust gas. The losses associated with the inlet and outlet of the channel are estimated as

$$\Delta P_{\mathrm{in/out}} = K_{\mathrm{in/out}} \times \frac{1}{2}\rho v^2,$$

where $K_{\mathrm{in/out}}$ is the inlet and outlet loss coefficients [30] which is given by

$$K_{\mathrm{in}} = -0.415 \times \mathrm{OFA} + 1.08$$

and

$$K_{\mathrm{out}} = (1 - \mathrm{OFA})^2,$$

where OFA refers to the open frontal area of the catalyst, i.e. the fraction of the frontal area that is open for the fluid to flow through. We combine the above expressions to give the pressure drop

$$\Delta P = \left(4f\frac{l}{d} + K_{\mathrm{in}} + K_{\mathrm{out}}\right) \times \frac{1}{2}\rho v^2. \tag{2.4}$$

2.3 Modified Breguet Range Equation

Given an aircraft's SFC, range (R), flight speed (V), lift to drag ratio (L/D) and maximum landing mass (MLW), the Breguet range equation can be used to calculate the fuel burn [3]. To calculate the fuel burn for an aircraft with ammonia based SCR, the Breguet range equation needs to be modified to account for the consumption of the reductant during flight.

For a certain emission index of NO_x (in grams of NO_x as NO_2 per kilogram of fuel), $EI(NO_x)$, the mass of NO_x emitted per second ($\dot{m}_{NO_x}$) is given by

$$\dot{m}_{NO_x} = EI(NO_x) \times \dot{m}_f,$$

where $\dot{m}_f$ is the fuel mass flow rate. The stoichiometric ratio for the SCR reactions is 1:1, hence $\dot{n}_{NH_3} = \dot{n}_{NO_x}$, where $\dot{n}_{NH_3}$ and $\dot{n}_{NO_x}$ are the molar flow rates of ammonia and NO_x, respectively. Therefore the mass flow rate of the reductant required is given by

$$\dot{m}_{Red} = \left[\frac{EI(NO_x) \times M_r^*(Red)}{M_r(NO_2)}\right] \times \dot{m}_f,$$

where $M_r(NO_2)$ is the molecular mass of NO_2 in g/mol and $M_r^*(Red)$ is the mass of reductant (in grams per mole of ammonia). The quantity in square parentheses is the fuel specific reductant consumption (FSRC).

For a given aircraft that is carrying fuel and reductant on board and using them at the rate of $\dot{m}_f$ and $\dot{m}_{Red}$ the rate of change of the aircraft mass $M_{a/c}$ can be expressed as

$$\frac{dM_{a/c}}{dt} = -(\dot{m}_f + \dot{m}_{Red}) = -\dot{m}_f\left(1 + \frac{\dot{m}_{Red}}{\dot{m}_f}\right) = -T \times SFC\left(1 + \frac{\dot{m}_{Red}}{\dot{m}_f}\right), \qquad (2.5)$$

where T is the thrust of the engine. We can re-write $T = \frac{gM_{a/c}}{L/D}$, where g is the

acceleration due to gravity. Eq 2.5 can then be rearranged and integrated as

$$\int_{M_{T/O}}^{\text{MLW}} \frac{dM_{a/c}}{M_{a/c}} = -g\frac{SFC}{L/D}\left(1 + \frac{\dot{m}_{\text{Red}}}{\dot{m}_f}\right)\int_0^{t_f} dt,$$

where $M_{T/O}$ is the take-off mass, MLW is the maximum landing weight and t_f is the flight time. This can be written in terms of the flight speed V, as

$$\int_{M_{T/O}}^{\text{MLW}} \frac{dM_{a/c}}{M_{a/c}} = -g\frac{SFC}{V \times L/D}\left(1 + \frac{\dot{m}_{\text{Red}}}{\dot{m}_f}\right)\int_0^{R} dx.$$

Carrying out the above integration and noting that $M_{T/O} = \text{MLW} + M_f(1 + \frac{\dot{m}_{\text{Red}}}{\dot{m}_f})$, we relate the mass of fuel required for a certain range (R) as,

$$M_f = \frac{\text{MLW}}{1 + \frac{\dot{m}_{\text{Red}}}{\dot{m}_f}}\left[\exp\left(gR\frac{\text{SFC}(1 + \frac{\dot{m}_{\text{Red}}}{\dot{m}_f})}{V \times L/D}\right) - 1\right]. \tag{2.6}$$

2.4 Estimating fuel burn penalty

To evaluate the fuel burn penalty associated with a certain level of NO_x removal we estimate the increase in SFC (due to the pressure drop) and landing mass of the aircraft (due to the mass of the SCR catalyst and reductant carried). We do not consider other changes in mass, assuming they are relatively small and that the change in mass occurs relative to some future design, e.g. a turbo-electric design. A gas turbine cycle deck is used to estimate the increase in SFC due to the pressure loss through the catalyst monolith. In this work we used a GasTurb 13 engine model provided by Pratt and Whitney to evaluate the impact on SFC due to a pressure drop downstream of the LPT.

The implications for three engines were assessed, a representative turbofan (110 kN (25000 lbf) thrust class), a geared turbofan for the same thrust class and a small core engine (58 kN (13000 lbf) thrust class). The comparitively lower thrust of the small core engine is due to higher L/D (≈ 20) [10] benefits from future airframes.

The GasTurb model is calibrated at the engine design operating point and the

effect of the pressure drop through the catalyst is modeled by varying the pressure drop in turbine exit duct in a series of off-design calculations. GasTurb was run iteratively such that the engine produces the same design point thrust for each turbine exit duct pressure drop by adjusting the combustor exit temperature. This directly corresponds to increasing the fuel flow rate and hence the SFC. Knowing the increase in the maximum landing mass and the increase in SFC, we can calculate the percentage increase in fuel burn using Eq (2.6).

We size the catalyst by first considering effective bulk dimensions as shown in Fig 2-2. Once the required effective size is determined we can pack the catalyst into a compact configuration. The catalyst for this purpose is characterized by three parameters – the catalyst substrate, total frontal area (A) of the catalyst and the reacting length (l) of each channel in the catalyst. The catalyst substrate sets the hydraulic diameter of each channel, the bulk density and the open frontal area (OFA) of the catalyst. A sets the local velocity of the flow in each channel by continuity and the reacting length of the channel sets the residence time of the exhaust gases within the catalyst.

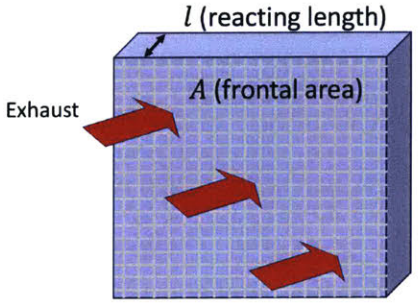

Figure 2-2: Bulk effective dimensions of the lumped catalyst model. Frontal area is defined as the area perpendicular to the flow through the catalyst.

The above three parameters also indirectly affect the SFC of the engine. Once values are chosen for the substrate, flow through area and the reacting length we compute the pressure drop and the NO_x conversion fraction. The pressure drop and additional weight is then used to calculate the increase in fuel burn from the baseline case (where no after treatment is used and no additional weight is carried).

2.5 Estimating air-quality benefits of post-combustion emissions control

The effect of reducing aviation NO_x through post-combustion emissions control, on ground level O_3 and $PM_{2.5}$ concentrations is estimated by using a global atmospheric chemistry and transport model.

GEOS-Chem Forward Model

The chemistry and transport of various chemical species is calculated by using the GEOS-Chem global atmospheric chemistry and transport model [5]. To capture the impact on stratospheric chemistry of aerosols and other species of interest, the GEOS-Chem UCX mechanism was employed [12]. The spatial resolution used is a 4° x 5° global grid, and 72 vertical layers (from sea-level to a pressure altitude of 0.01 hPa). GEOS-Chem solves global chemistry and transport equations to calculate global spatial and temporal distribution of chemical species.

Table 2.1: GEOS-Chem simulation scenarios. Each scenario has different emission cases.

Scenario	Description
1: NonAv	All anthropogenic emissions except aviation
2: AllSources	All anthropogenic emissions including aviation
3: PCEC	All anthropogenic emissions including aviation with post-combustion emissions control (PCEC)
4: PCEC+ULS	All anthropogenic emissions including aviation with post-combustion emissions control (PCEC) and ultra-low sulfur (ULS) fuel

Four simulations of one year duration each, were carried out for different scenarios that were then used to isolate the impact of post-combustion emissions control on air-quality. The scenarios are described in table 2.1. Default GEOS-Chem inventories like the EDGAR v4.2 global anthropogenic emissions inventory [13] were used for all scenarios. Senarios 1 (NonAv) and 2 (AllSources) were run without and with the Aviation Environmental Design Tool (AEDT) respectively. Scenarios 3 (PCEC) and 4 (PCEC+ULS) were computed by modifying aviation emissions to account for

post-combustion emissions control and ultra-low sulfur jet fuel respectively. This was done by appropriately scaling down aviation NO_x emissions and introducing ammonia emissions (NH_3) to capture the effect of ammonia slip in scenario 3 (PCEC). Fuel sulfur content was reduced from 600 ppm (typical jet fuel) to 15 ppm in scenario 4 (PCEC+ULS) in addition to scaling down NO_x and introducing NH_3 emissions. Weighting the annual average ground level concentration of $PM_{2.5}$ with the global population density (using LandScan 2015 population distribution) gives the effective $PM_{2.5}$ exposure.

Chapter 3

Results and Discussion

Applying the methods outlined in the previous section, we obtain an estimate of the effectiveness of post-combustion emissions control for NO_x reduction in aircraft gas turbine engines. The results shown here are for a geared turbofan configuration (state of the art technology) with the SCR catalyst installed downstream of the LPT unless otherwise specified. The core exhaust is assumed to be accelerated downstream of the catalyst in a propelling nozzle to produce thrust. However, we envision that the actual application of post-combustion emissions control with a clean-sheet engine and aircraft design may be configured so that all the thrust is delivered by separate propulsors. This may be in a turbo-electric configuration or by mechanical transmission as in a tubroprop engine.

3.1 Mass transfer limited regime

To verify that the catalyst is indeed operating in the mass transfer limited regime we calculate the Damköhler number

$$\mathrm{Da} = \frac{k_c d}{D_{\mathrm{NO}}},$$

where k_c is the rate constant for the chemcial reaction [37] and D_{NO} is the diffusivity of NO at a particular temperature and pressure which is calculated based on values form

Tang et al [34]. At high temperatures (450 °C) the catalytic reactions are confined to a very thin layer (5-10 μm) of the wash-coat [21] thus the effective diffusivity of the reactants can be treated as approximately equal to the binary diffusion coefficient, i.e. $(D_{\text{eff}})/(D) \approx 1$. However, we conservatively choose $D_{\text{eff}} \approx D/3$ to account for any inaccuracies introduced by the lumped parameter model. At the temperatures and pressures found downstream of the LPT, we find Da $\approx 1.6 \times 10^{10}$, which indicates that the chemical reactions are several orders of magnitude faster than the mass transfer from the free stream to the wall.

DeNO_x is thus only dependent on $z^* = (zD_{\text{NO}})/(ud^2)$. Thus the required residence time ($\tau = z/u$) for a certain level of DeNO_x is dependent only on the square of the hydraulic diameter of the channel, d^2 (for a given diffusivity D_{NO}). A smaller channel diameter implies a shorter residence time is required as compared to a larger channel diameter (see Fig 3-1).

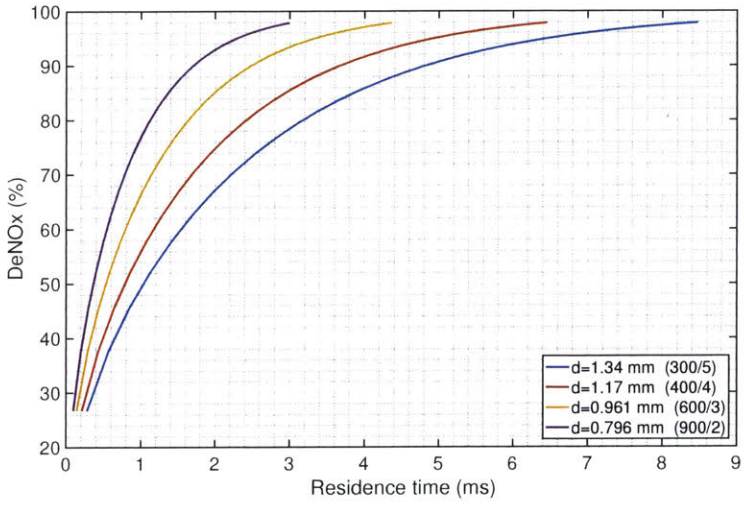

Figure 3-1: DeNO_x against τ for different channel hydraulic diameters. 300/5 refers to a catalyst substrate of 300 cells per square inch (cpsi) with a wall thickness of 5 mil, which is the conventional way of characterizing the catalyst substrate geometry.

3.2 Estimating fuel specific reductant consumption

The fuel-specific reductant consumption for various reductants is calculated based on X_{m,NH_3} and an average cruise EI(NO_x) of 14 g/kg [2] and tabulated in Table 1.1. We see that pure anhydrous liquid ammonia has the lowest reductant consumption as it has the highest ammonia content per unit mass. We note that post-combustion emissions control is also applicable to the landing and takeoff cycle, but here we consider the cruise EI(NO_x) as this dominates NO_x emissions and corresponding reductant consumption.

3.3 Effect of catalyst size on DeNO$_x$ and fuel burn penalty

The effect of catalyst size on DeNO$_x$ and the associated fuel burn penalty is shown in Fig 3-2. The reacting length was fixed at 1.25 cm in this analysis as this results in a packed size that could fit in two of the typical seven containers of the cargo hold in an A320 aircraft.

The gas hourly space velocity (GHSV) is defined as the ratio of the volume flow rate per hour of the exhaust gas to the bulk volume of the catalyst and is inversely proportional to the the residence time in the catalyst. A large catalyst corresponds to a smaller GHSV (longer residence time) and hence shows a greater conversion of NO_x. Fig 3-2 shows that post-combustion emissions control as evaluated here has the potential to reduce the NO_x emissions by over 95% for approximately a 0.4% increase in fuel burn. The GHSV at which this conversion is achieved is approximately 1×10^6 h^{-1}, which is in the same order of space velocity encountered in the heavy duty diesel industry during peak load operation. The catalyst total frontal area required for this conversion is approximately 19 m^2.

The average DeNO$_x$ during the LTO cycle is approximately 75% due to the higher pressures at lower altitudes which decreases the effective diffusivity (D_{eff}) of the reacting species. However, according to Yim et al. [41], cruise emissions account for

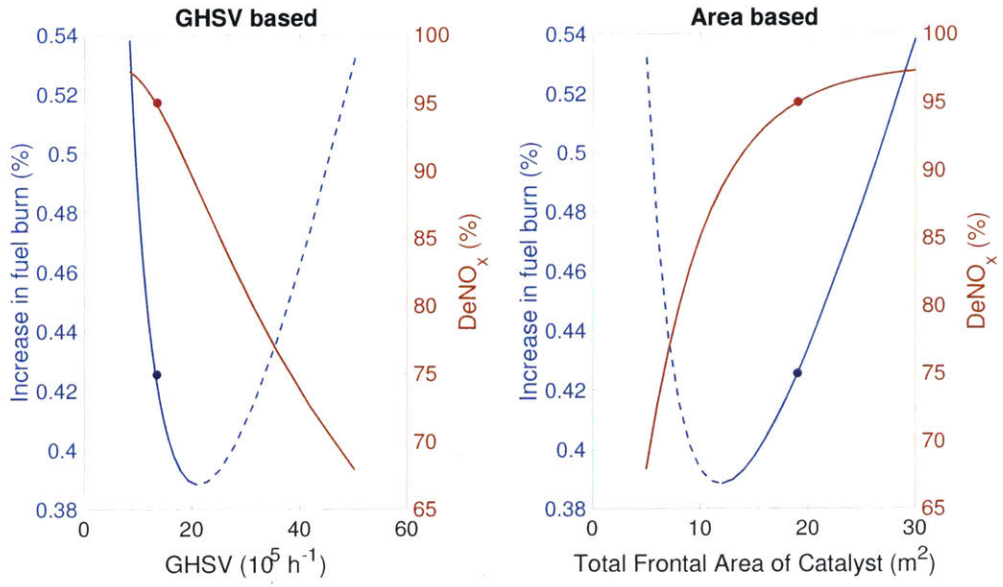

Figure 3-2: Tradeoff between catalyst size and performance shown on two different basis. **Left:** Effect of GHSV on $DeNO_x$ and fuel burn penalty. **Right:** Effect of flow through area on $DeNO_x$ and fuel burn penalty. Chosen design point is marked with by solid circles. Solid portion of the fuel burn curve represents the desirable region of operation where the catalyst efficiency is high, while the dashed portion of the curve represents an undesirable operating region.

three-quarters of the premature mortalities attributable to aviation $PM_{2.5}$ and ozone. The $DeNO_x$ during cruise is higher ($\sim$97%) which results in an effective $DeNO_x$ of $\sim$95% over the full flight (a 1500 km range mission is studied here). Reduction in the conversion efficiency while the catalyst warms up has not been accounted for and needs to be further investigated.

This approach highlights the competing effects of pressure drop and increasing mass of the catalyst. As the size of the catalyst is increased the pressure drop incurred can be reduced (decreasing fuel burn). However, this comes at the cost of additional weight (increasing fuel burn). This tradeoff is elucidated by the graph on the right in Fig 3-2, as the frontal area of the catalyst is increased from approximately 5 m^2 to approximately 10 m^2 the fuel burn penalty decreases. This is a direct consequence of the lower flow velocity and hence smaller pressure drop downstream of the LPT. Further increase in the flow through area results in an increase in fuel burn penalty. This behavior can be explained by the catalyst mass, which affects the maximum

landing mass of the aircraft and hence the fuel required to fly the same mission.

This is further supported by the data in Fig 3-3. The dashed blue lines show that as the reacting length (l) is decreased for a fixed catalyst frontal area (A) the pressure drop and the catalyst volume (and hence catalyst mass) decrease. This causes the $DeNO_x$ and fuel burn penalty to monotonically decrease. However, if l is held constant and A is increased, the pressure drop decreases but the catalyst mass increases. This causes the fuel burn penalty to first decrease and then increase as explained àbove. Higher lift to drag ratios (L/D) airframes will mitigate the impact that this additional weight has on the fuel burn penalty. This is seen from the modified range equation (Eq 2.6).

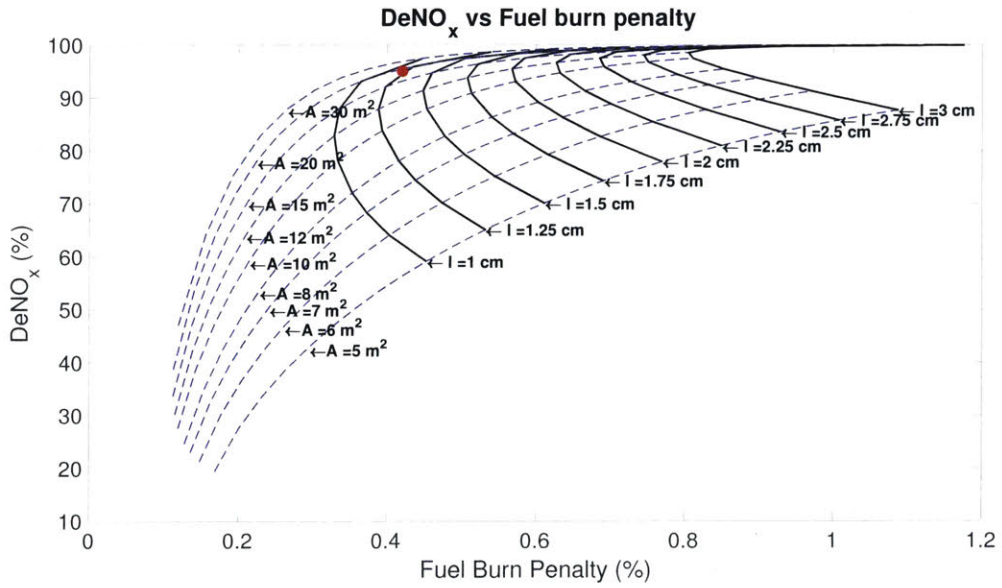

Figure 3-3: Tradeoff between $DeNO_x$ and fuel burn penalty. Each dashed blue lines show effect of changing reacting length (l) for a fixed frontal area (A). Solid black lines show the effect of changing frontal area while holding the reacting length constant. Design point is marked by red dot.

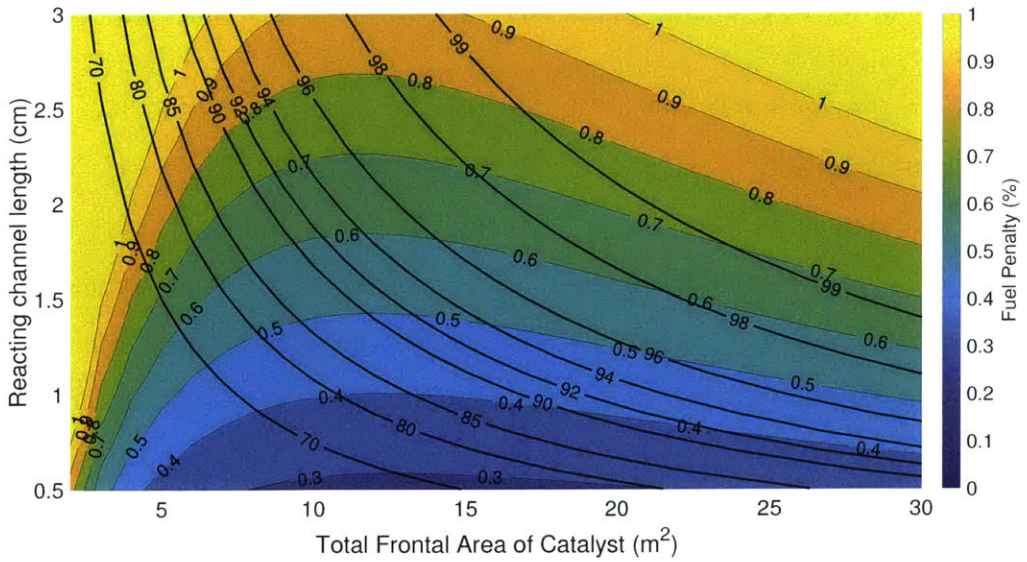

Figure 3-4: Tradeoff between $DeNO_x$ and fuel burn penalty as a function of catalyst bulk geometry. The colored contours show the fuel burn penalty. The solid black lines represent $DeNO_x$ as a percentage.

3.4 Trade off between $DeNO_x$, ammonia slip, and fuel burn penalty

Emissions of unreacted ammonia, referred to as ammonia slip, can be quantified using the stoichiometric ratio of the SCR reaction. In some designs, a catalyst is introduced downstream of the SCR to oxidize any unreacted ammonia in the exhaust stream. More advanced designs have been proposed where the monolith substrate is coated in layers of different catalytic materials which minimizes ammonia slip.

Fig 3-4 shows the tradeoff between $DeNO_x$ and fuel burn penalty when the reacting length and the flow through area are varied. For a reacting length of approximately 1.25 cm and a total frontal area of 19 m^2 we can achieve a 95% reduction in NO_x emissions for approximately a 0.4% increase in fuel burn. Calculating the average ammonia slip in terms of an emission index gives an $EI(NH_3)$ of approximately 0.26 g NH_3/kg fuel.

While ammonia slip at ground level results in the formation of $PM_{2.5}$ which adversely affects human health [8], cruise altitude emissions of ammonia do not share

the same immediate risk, since neither the ammonia nor its products would reach population at ground level due to the atmospheric transport phenomenon at cruise altitude. As identified by Eastham et al. [11] the mixing of aviation attributable ozone from cruise altitude is the mechanism responsible for exposure to both ozone and $PM_{2.5}$. This is further supported by the analysis presented in section 3.8.

3.5 Effect of engine core size on post-combustion emissions control

The NASA N+3 aircraft concept design and trade studies final report [16] indicates that the aircraft industry is exploring small core, high efficiency engines that are employed along with other advance configurations such as blended wing bodies, boundary layer ingestion and distributed propulsion [26, 10, 16]. We evaluate the impact that a small core engine architecture would have with regards to the use of post-combustion emissions control as outlined in this work.

Fig 3-5 shows the results of evaluating the after treatment methods on three different engine architectures. The conventional turbofan is representative of a modern mixed flow turbofan, the geared turbofan represents the state of the art low fan pressure ratio geared turbofans, and the small core engine is representative of an advanced engine architecture that was proposed to be used on the MIT D8 aircraft [26]. The envisioned application of post-combustion emissions control as described in this work is on turbo-electric configurations, potentially with distributed propulsion.

We see from Fig 3-5 that the performance of the post-combustion control system improves as the core size decreases. Considering the core size (expressed as the corrected mass flow at compressor exit), current generation engines have a core size of 3.18 kg/s (7 lb/s), geared turbofans have a core size of 2.27 kg/s (5 lb/s) and the next generation engines are likely to have an even smaller core size of 0.68 kg/s (1.5 lb/s) [26]. The thrust size for the conventional and geared turbofan engines is 110 kN (25000 lbf) and the small core engine has the above core size at 58 kN (13000 lbf).

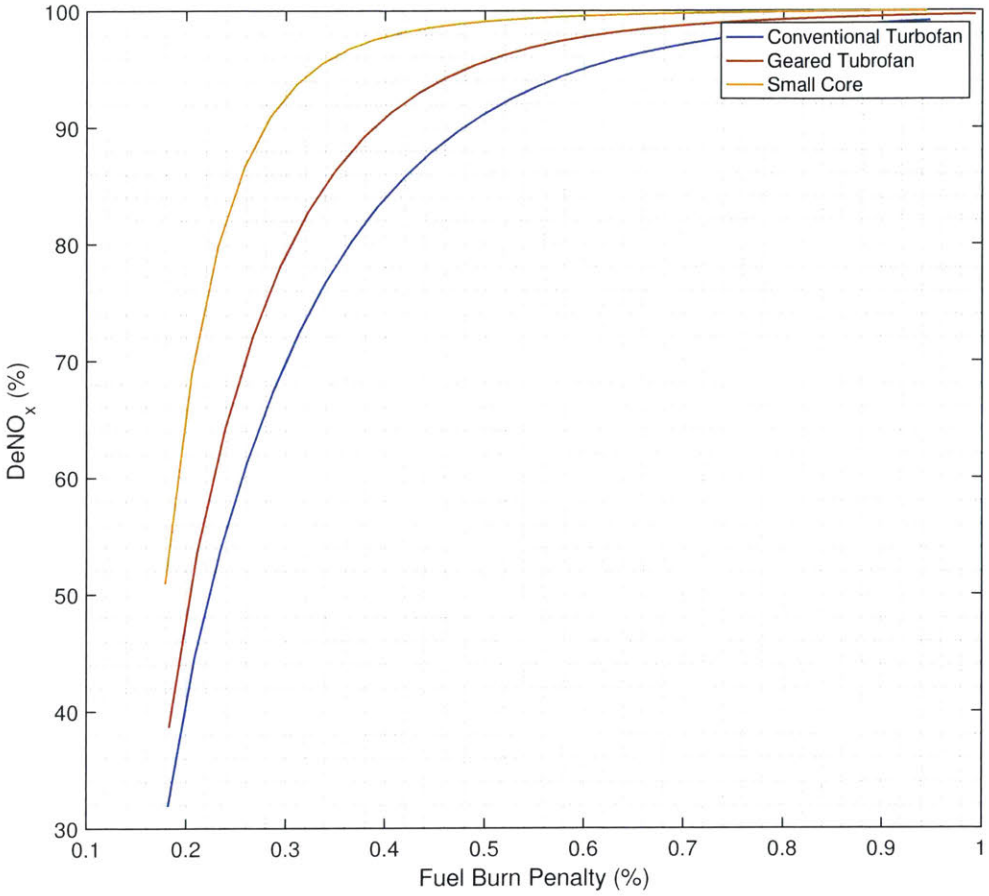

Figure 3-5: Post-combustion emissions control applied to different engine architectures.

The small core engine has a lower thrust rating since the envisioned airframe has a higher L/D of approximately 20 [10].

We can explain this trend by estimating the sensitivity of the fuel burn increase to the catalyst mass and geometry.

Using the modified range equation 2.6, we calculate the sensitivity of the fuel burn to the catalyst weight ($\frac{\partial M_f}{\partial \mathrm{MLW}}$) as

$$\frac{\partial M_f}{\partial \mathrm{MLW}} = \frac{1}{1+\frac{\dot{m}_{\mathrm{Red}}}{\dot{m}_f}}\left[\exp\left(gR\frac{\mathrm{SFC}(1+\frac{\dot{m}_{\mathrm{Red}}}{\dot{m}_f})}{V\times L/D}\right)-1\right], \tag{3.1}$$

and the sensitivity of fuel burn to the pressure drop ($\frac{\partial M_f}{\partial \Delta P}$) as

$$\frac{\partial M_f}{\partial \Delta P} = \frac{\partial M_f}{\partial \text{SFC}} \times \frac{\partial \text{SFC}}{\partial \Delta P}, \tag{3.2}$$

where

$$\frac{\partial M_f}{\partial \text{SFC}} = \frac{\text{MLW} g R}{V \times L/D} \exp\left(gR \frac{\text{SFC}(1 + \frac{\dot{m}_{\text{Red}}}{\dot{m}_f})}{V \times L/D}\right). \tag{3.3}$$

The sensitivities for the different engines are calculated and tabulated in Table 3.1.

Table 3.1: Sensitivity of M_f to the mass of the catalyst and the pressure drop induced by the catalyst. ΔP is the pressure drop through the catalyst

Engine	$\frac{\partial M_f}{\partial \text{MLW}}$	$\frac{\partial M_f}{\partial \text{SFC}}$	$\frac{\partial \text{SFC}}{\partial \Delta P}$	$\frac{\partial M_f}{\partial \Delta P}$
-	(kg/kg)	(kg/(kg/Ns))	((kg/Ns)/kPa)	(kg/kPa)
Conventional Turbofan	0.0695	2.72×10^8	9.87×10^{-8}	26.8
Geared turbofan	0.0542	2.68×10^8	1.13×10^{-7}	30.3
Small core engine	0.0532	2.67×10^8	1.35×10^{-7}	36.2

We note that the sensitivity of SFC to the pressure drop increases as the core size decreases which increases the sensitivity of the fuel burn to the pressure drop. However, the sensitivity of fuel burn to landing mass and SFC decreases as the core size decreases. This provides evidence to indicate that the target design space should minimize the pressure drop by increasing the frontal area (A) of the catalyst, even though this comes at the cost of increased mass.

$DeNO_x$ only depends on the residence time, which is set by the volume of the catalyst. The pressure drop and consequently the SFC of the engine depends on the geometry of the catalyst. Equations 3.1, 3.2 and 3.3 represent the sensitivity of fuel burn to catalyst mass and pressure drop. The equations show that the fuel penalty decreases as the baseline SFC decreases and the airframe L/D increases, as can be expected from future designs being proposed [10, 26, 16]. Furthermore for a fixed catalyst size, as the core mass flow of the engine decreases the pressure drop through the catalyst decreases since the flow velocity decreases which provides additional performance benefits.

The author envisions the proposed post-combustion emissions control methods could be implemented in tandem with a small core architecture that could be housed within the body of the aircraft in a turbo-electric configuration or possibly with a decoupled propulsor such as in the D8 aircraft [26]. This could allow installation of the catalyst in the belly of the aircraft. The core flow in such a design would thus contribute no thrust, although the design may be configured such that the core intake ingests the airframe boundary layer, providing scope for further improvement of the post-combustion emissions control performance.

3.6 Packing Constraints

The results above shows that a catalyst of 19 m^2 in frontal area and 1.25 cm in thickness is required for $DeNO_x \approx 95\%$. The packaging of this catalyst into the airframe may not be possible with a "flat" catalyst configuration as shown in Fig 2-2. An air-filter like pleated design allows us to pack a large area catalyst into a small packing volume. An illustration is shown in Fig 3-6, where the flow enters axially and leaves radially. As shown in Appendix A, a pleated design with internal radius r, pleat depth h, N pleats, reacting length l, and total length L, surface area of the interior is given by

$$A = 2NL\sqrt{h^2 + \frac{r^2}{2}(1 - \cos(2\pi/N)) - l^2}. \tag{3.4}$$

Applying Eq 3.4 shows that we can fit this area of catalyst into a cylinder of length 2.2 m and outer diameter of 1 m (using 24 pleats and a pleat depth of 18 cm). Detailed analysis concerning the packing and manufacturing of the catalyst design will be subject of future research.

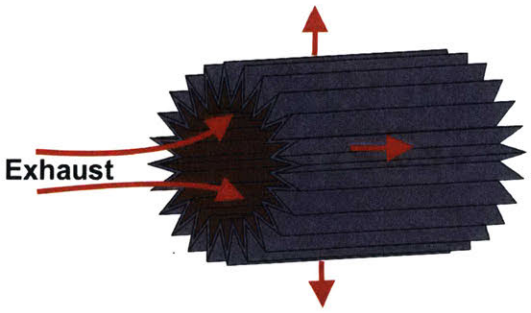

Figure 3-6: Illustration of pleated catalyst design to pack large area catalyst into the belly of an aircraft

3.7 Sulfur content and catalyst fouling

A consideration in the use of SCR is that sulfur content in the fuel can lead to catalyst fouling, which results in the deactivation of the catalytic sites and subsequent loss of catalytic performance. The sulfur content in the fuel needs to be less than 15 ppm as is the case for ultra-low sulfur diesel fuel that is used on road vehicles [1]. Studies on the economics and costs of desulfurizing jet fuel has been previously carried out by Barrett et al. [4]. According to Eastham et al [11] ~57.5% of aviation-attributable premature mortalities were due to $PM_{2.5}$ and ~42.5% were attributable to ozone, where the ozone impacts are due to NO_x emissions in the upper troposphere and lower stratosphere. Yim et al [41] show that approximately 97% of the $PM_{2.5}$ consists of secondary particulate matter formed by NO_x and SO_x, and 3% is primary $PM_{2.5}$. Furthermore, Koo et al [22], show that approximately 93% of secondary $PM_{2.5}$ was due to NO_x and 7% was due to SO_x.

Hence by using post-combustion emissions control (~95 % $DeNO_x$ in tandem with desulfurized (15 ppm fuel sulfur content i.e. 97.5% reduction in SO_x) jet fuel, we may avert as many as ~92% of the premature mortalities attributable to aviation emissions. This estimate is further supported by calculations using a global chemistry and transport model (GEOS-Chem).

3.8 Air-quality impacts due to post-combustion emissions control

The GEOS-Chem model is used to estimate the air-quality benefits of applying post-combustion emissions control to aviation. Figure 3-7 shows the effect that post-combustion emissions control has on $PM_{2.5}$ at different altitudes. The solid black curve indicates the baseline $PM_{2.5}$ concentration attributable to aviation. The dashed blue line (with post-combustion emissions control) shows that there is a decrease in $PM_{2.5}$ concentrations at almost all altitudes despite any ammonia slip. This supports the earlier claim in 3.4 that any $PM_{2.5}$ formed at altitude, due to reaction of NH_3 and residual NO_x, is wet deposited and does not pose a health hazard to population. The solid blue line, shows the $PM_{2.5}$ concentration resulting from post-combustion emissions control and desulfurized fuel.

Using the ground level $PM_{2.5}$ concentrations as shown in Fig 3-8 and population density, the annual average population exposure to $PM_{2.5}$ is calculated for the two scenarios (business as usual and desulfurized jet fuel with post-combustion emission control employed). Post-combustion emissions control along with desulfurized jet fuel leads to approximately 91.5% reduction in annual global average population exposure to $PM_{2.5}$.

A similar calculation is carried out using the forward model for ground level ozone concentration and column ozone as shown in figures 3-9 and 3-10. The average reduction in population exposure to ozone is approximately 95%. While reducing ground level ozone concentration has a health benefit, a reduction in column ozone can increase the risk of melanoma. However as estimated by Eastham et al [11] the avoided mortalities due to melanoma resulting from column ozone created by aviation is small compared to the total mortalities attributable to aviation.

Thus, a 91.5% reduction in $PM_{2.5}$ exposure and 95% reduction in ozone exposure suggests that desulfurized jet fuel used in tandem with post-combustion emissions control could reduce $\sim$93% of aviation attributable premature mortalities.

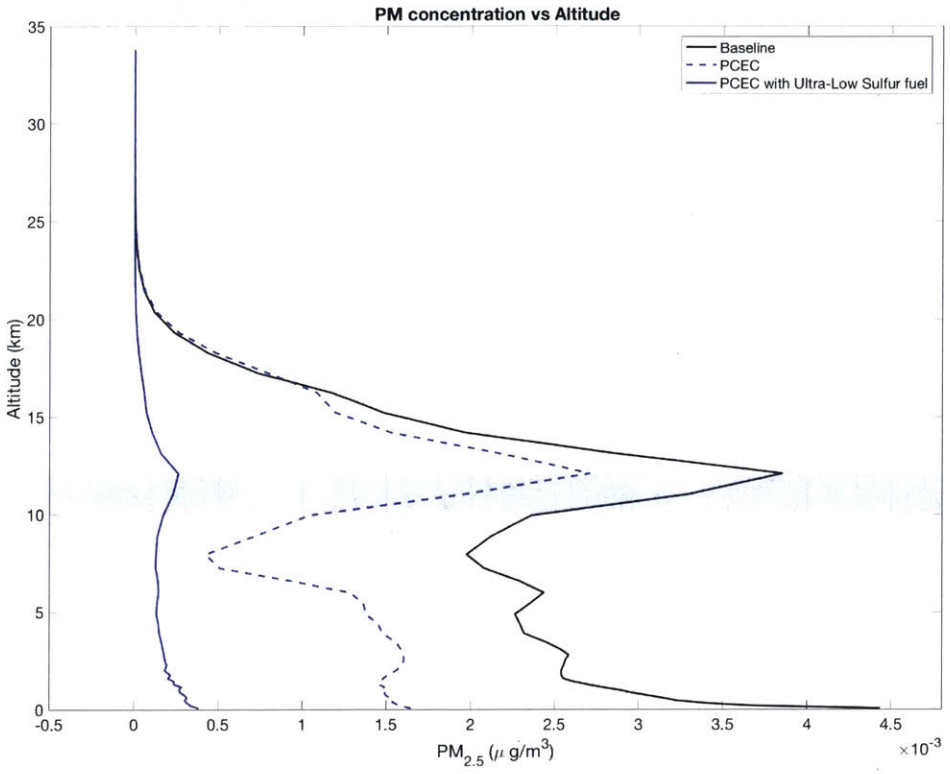

Figure 3-7: Annual average $PM_{2.5}$ concentration vs Altitude resulting from post-combustion emissions control (PCEC). $PM_{2.5}$ concentrations are averaged across latitude and longitude for each altitude. The light blue box indicates typical cruise altitude for commercial aviation.

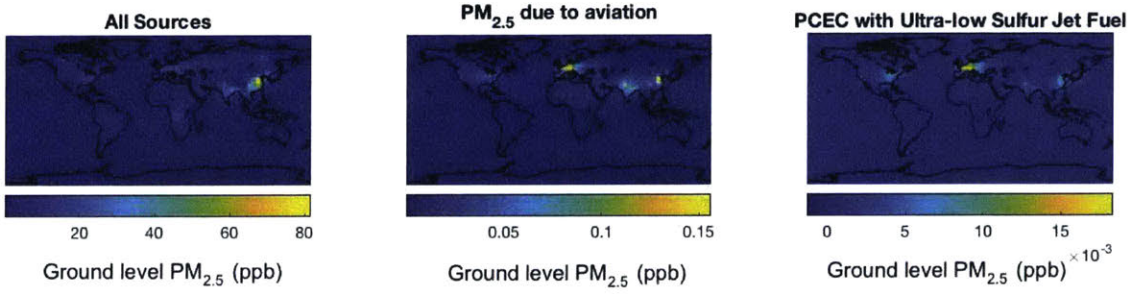

Figure 3-8: Annual average ground level $PM_{2.5}$ concentration in ppb

3.9 Selective non-catalytic reduction of NO_x

It has been observed that under a narrow temperature range, an ammonia based reducing agent can reduce the nitrogen oxides without the presence of a catalyst [32, 35]. This process is referred to as selective non-catalytic reduction (SNCR).

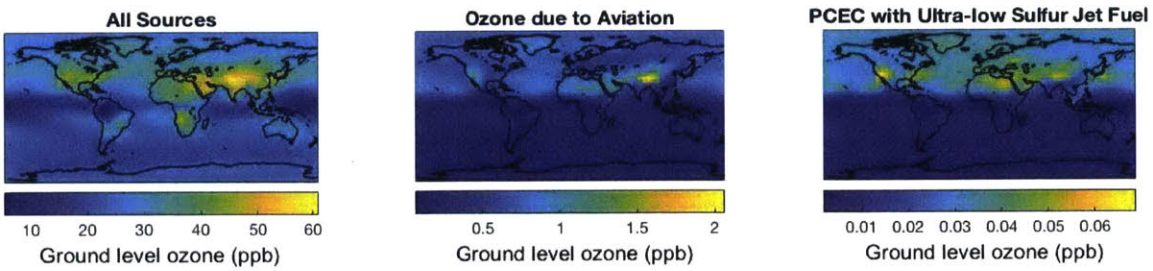

Figure 3-9: Annual average ground level ozone concentration in ppb.

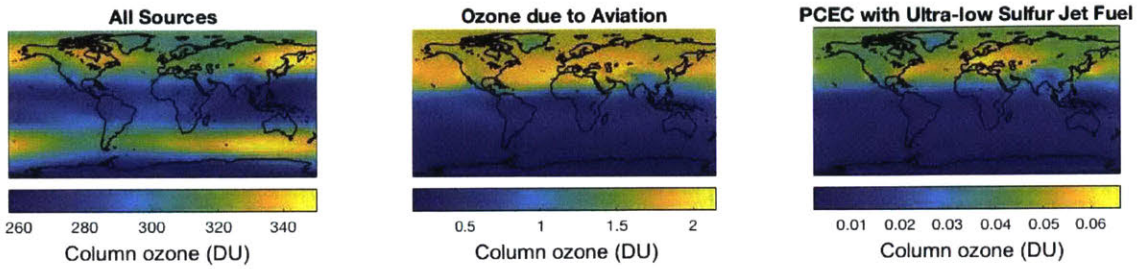

Figure 3-10: Annual average column ozone in Dobson units (DU)

Thus spraying the ammonia in the inter-turbine duct or another suitable location where the temperature range is 1100 to 1400 K [25, 27], leads to additional NO_x reduction through this non-catalytic pathway. Analysis using Cantera [15], based on the mechanism proposed in [32] shows that for typical flow velocities in the inter turbine duct we get approximately a 2.6% reduction in NO_x as shown in the Appendix. Thus the mass of NO_x entering the catalyst is 98% of the original combustor out mass of NO_x of which approximately 95% is reduced catalytically in the catalyst. This additional conversion has not been considered in the above quoted performance of the catalytic reduction, given the predominance of the SCR.

Chapter 4

Conclusions

This work is the first proposal and assessment of post-combustion emissions control techniques for aircraft gas turbine engines and evaluates the case for the use of selective catalytic reduction for NO_x control in the aviation sector. The analytical approach, built upon prior work done in SCR applications for diesel engines shows that a 95% reduction in NO_x emissions can be achieved for approximately a 0.4% increase in fuel burn. The sensitivity of the fuel burn to catalyst mass and catalyst induced pressure drop show that the performance of the emissions control system improves for future designs where smaller core sizes, higher engine efficiency and higher L/D airframes are expected. Furthermore optimization and improvements in catalyst technology will further improve the performance of post-combustion emissions control.

The size of the catalyst to achieve this level of conversion implies the likely need to be housed in the body of the aircraft. A NASA N+3 aircraft design such as the D8 with small core engines, and turbo-electric designs, may offer further potential for optimization. Additionally using post-combustion emissions control to reduce NO_x could result in combustor design space benefits that improve combustor efficiency. Using GEOS-Chem – a global chemistry and transport model, it is estimated that approximately 93% of air pollution impacts of aviation could be averted with the use of post-combustion emissions control in tandem with desulfurized jet fuel. Further work is required to evaluate the detailed environmental and economic costs and benefits of

reducing NO_x emissions by 95%. In addition assessment of the aircraft configurations (turbo-electric, small core engine etc.) and specific design concepts are needed.

Appendix A

Surface area of pleated geometry

This section provides the derivation of Eq 3.4. The total surface area (A) seen by the flow is given by

$$A = 2NL \times s,$$

where N is the number of pleats, L is the total length of the catalyst (perpendicular to the paper) and s is the length of the line segment AB as shown in Fig A-1. The length s is given by

$$s = \sqrt{x^2 - l^2}$$

and

$$x^2 = h^2 + \frac{r^2}{2}(1 - \cos(2\pi/N)),$$

where r is the internal radius as shown in Fig A-1. Therefore the total internal area seen by the flow is given by

$$A = 2NL\sqrt{h^2 + \frac{r^2}{2}(1 - \cos(2\pi/N)) - l^2}.$$

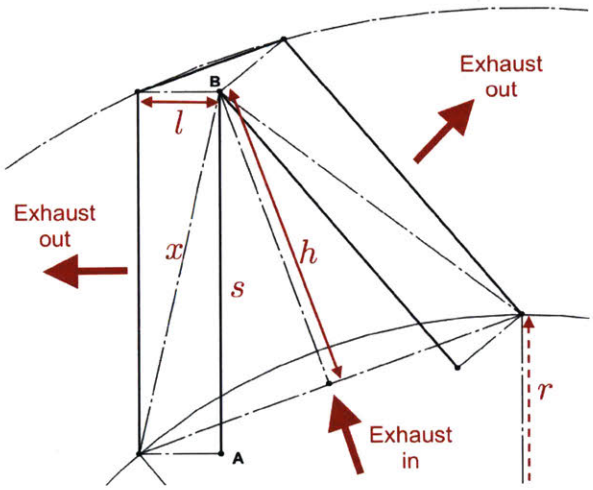

Figure A-1: Geometry of pleated catalyst design. Only one pleat is shown here. The reacting length and the pleat depth are l and h respectively. The radius of the inner circle is r and the length of the line segment AB is equal to s, this represents the actual flow through area per unit length perpendicular to the paper.

Appendix B

Selective non-catalytic reduction

As outlined in the main text ammonia reacts with NO_x in the temperature range of 1100 to 1400 K without the presence of a catalyst. CANTERA was used to model selective non-catalytic reduction (SNCR) of ammonia with NO_x and the reaction mechanisms reported by Chang [32] were used. Two reactors were setup in CANTERA, the first to model the inter-turbine duct and the second to model the reactions in the low pressure turbine. The mixture state in the second reactor was calculated using the end state of the first reactor and assuming a lumped isentropic expansion in the low pressure turbine. The results from these simulations are shown in Fig B-1. We note that the SNCR reactions result in approximately a 2.6% $DeNO_x$. We see the discontinuity in the graph at 0.4 ms, where the gases are reacting in the second reactor. The temperatures and pressures are lower after expansion in the low pressure turbine which is results in lower consumption rates of ammonia and NO_x. The contribution of SNCR related $DeNO_x$ was not considered in the main text because the $DeNO_x$ due to SCR dominates the overall reduction of NO_x from the exhaust stream.

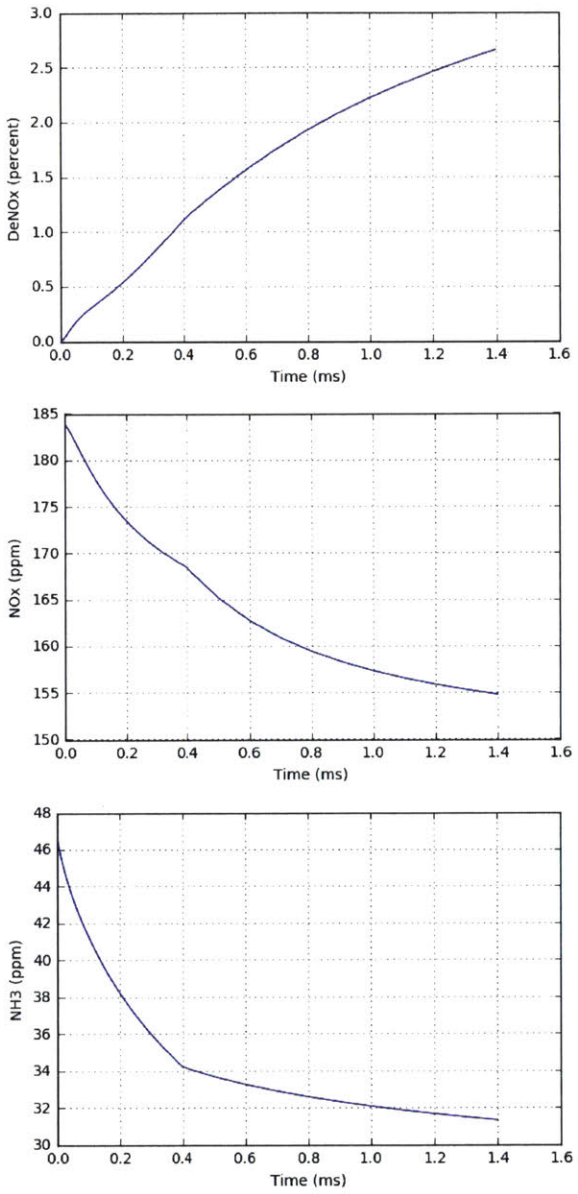

Figure B-1: Results of SNCR simulation using Cantera

Bibliography

[1] Environmental Protection Agency Control of Air Pollution From New Motor Vehicles: Heavy-Duty Engine and Vehicle Standards and Highway Diesel Fuel Sulfur Control Requirements;. Technical Report 12, 2001.

[2] ICAO Aircraft Engine Emissions Databank. http://www.easa.europa.eu/document-library/icao-aircraft-engine-emissions-databank, 2017. Version 24.

[3] John Anderson. *Introduction to Flight.* McGraw-Hill Higher Education, 2015.

[4] Steven R H Barrett, Steve H L Yim, Christopher K. Gilmore, Lee T. Murray, Stephen R. Kuhn, Amos P K Tai, Robert M. Yantosca, Daewon W. Byun, Fong Ngan, Xiangshang Li, Jonathan I. Levy, Akshay Ashok, Jamin Koo, Hsin Min Wong, Olivier Dessens, Sathya Balasubramanian, Gregg G. Fleming, Matthew N. Pearlson, Christoph Wollersheim, Robert Malina, Saravanan Arunachalam, Francis S. Binkowski, Eric M. Leibensperger, Daniel J. Jacob, James I. Hileman, and Ian A. Waitz. Public health, climate, and economic impacts of desulfurizing jet fuel. *Environmental Science and Technology*, 46(8):4275–4282, 2012.

[5] Isabelle Bey, Daniel J. Jacob, Robert M. Yantosca, Jennifer A. Logan, Brendan D. Field, Arlene M. Fiore, Qinbin Li, Honguy Y. Liu, Loretta J. Mickley, and Martin G. Schultz. Global modeling of tropospheric chemistry with assimilated meteorology: Model description and evaluation. *Journal of Geophysical Research: Atmospheres*, 106(D19):23073–23095, oct 2001.

[6] Boeing Commercial Airplanes Market Analysis. Current Market Outlook 2016-2035. www.boeing.com/cmo, 2016.

[7] Henry Cohen, G. F. C. Rogers, and H. I. H. Saravanamuttoo. *Gas Turbine Theory.* Longman Pub Group, 1996.

[8] Douglas W. Dockery, C. Arden Pope, Xiping Xu, John D. Spengler, James H. Ware, Martha E. Fay, Benjamin G. Ferris, and Frank E. Speizer. An Association between Air Pollution and Mortality in Six U.S. Cities. *New England Journal of Medicine*, 329(24):1753–1759, 1993.

[9] Christopher S. Dorbian, Philip J. Wolfe, and Ian A. Waitz. Estimating the climate and air quality benefits of aviation fuel and emissions reductions. *Atmospheric Environment*, 45(16):2750–2759, 2011.

[10] Mark Drela. Development of the D8 Transport Configuration. *29th AIAA Applied Aerodynamics Conference*, (June):27–30, 2011.

[11] Sebastian D. Eastham and Steven R H Barrett. Aviation-attributable ozone as a driver for changes in mortality related to air quality and skin cancer. *Atmospheric Environment*, 144:17–23, nov 2016.

[12] Sebastian D. Eastham, Debra K. Weisenstein, and Steven R.H. Barrett. Development and evaluation of the unified tropospheric–stratospheric chemistry extension (UCX) for the global chemistry-transport model GEOS-chem. *Atmospheric Environment*, 89:52–63, jun 2014.

[13] Joint Research Centre (JRC)/Netherlands Environmental Assessment Agency (PBL) European Commission. Emission Database for Global Atmospheric Research (EDGAR). http://edgar.jrc.ec.europa.eu, 2011. Release version 4.2.

[14] Gary Fulks, Galen B . Fisher, Ken Rahmoeller, Ming-Cheng Wu, Eric D'Herde, and Julian Tan. A Review of Solid Materials as Alternative Ammonia Sources for Lean NOx Reduction with SCR. *SAE Technical Paper*, 2009.

[15] David G. Goodwin, Harry K. Moffat, and Raymond L. Speth. Cantera: An object-oriented software toolkit for chemical kinetics, thermodynamics, and transport processes. http://www.cantera.org, 2017. Version 2.3.0.

[16] E. M Greitzer, P. A. Bonnefoy, E. De La Rosa Blanco, C. S. Dorbian, M. Drela, D. K. Hall, R. J. Hansman, J. I. Hileman, R. H. Liebeck, J. Lovegren, P. Mody, J. A. Pertuze, S. Sato, Z. S. Spakovszky, C. S. Tan, J. S. Hollman, and K. D. N + 3 Aircraft Concept Designs and Trade Studies , Final Report Volume 1. https://ntrs.nasa.gov/archive/nasa/casi.ntrs.nasa.gov/20100042401.pdf, 2010.

[17] Michael P. Harold and Pranit Metkar. Lean NOx reduction by NH3 on fe-exchanged zeolite and layered fe/cu zeolite catalysts: Mechanisms, kinetics, and transport effects. In *Urea-SCR Technology for deNOx After Treatment of Diesel Exhausts*, pages 311–356. Springer New York, 2014.

[18] Hannu Jääskeläinen and Magdi K Khair (Eds.). DieselNet Technology Guide: Diesel Engines. https://www.dieselnet.com/tech/diesel_engines.php, 2013.

[19] Timothy V. Johnson. Review of selective catalytic reduction (SCR) and related technologies for mobile applications. In *Urea-SCR Technology for deNOx After Treatment of Diesel Exhausts*, pages 3–31. Springer New York, 2014.

[20] Marilena Kampa and Elias Castanas. Human health effects of air pollution. *Environmental Pollution*, 151(2):362–367, 2008.

[21] M. Koebel, M. Elsener, and M. Kleemann. Urea-SCR: a promising technique to reduce NOx emissions from automotive diesel engines. *Catalysis Today*, 59(3):335–345, 2000.

[22] Jamin Koo, Qiqi Wang, Daven K. Henze, Ian A. Waitz, and Steven R H Barrett. Spatial sensitivities of human health risk to intercontinental and high-altitude pollution. *Atmospheric Environment*, 71(x):140–147, 2013.

[23] Arthur Lefebvre. *Gas Turbine Combustion.* Taylor & Francis, 1983.

[24] Arthur H. Lefebvre. Fuel effects on gas turbine combustion. *International Journal of Turbo and Jet-Engines*, 21(11):231 – 243, 1986.

[25] Tim C Lieuwen and Vigor Yang. *Gas turbine emissions.* Cambridge university press, 2013.

[26] Wesley K. Lord, Gabriel Suciu, Jesse Chandler, and Karl Hasel. Engine Architecture for High Efficiency at Small Core Size. *53rd AIAA Aerospace Sciences Meeting*, (January), 2015.

[27] Richard K. Lyon. Thermal DeNOx controlling nitrogen oxides emissions by a noncatalytic process. *Environmental Science & Technology*, 21(3):231–236, mar 1987.

[28] W Addy Majewski. Dieselnet technology guide: Catalyst fundamentals. https://www.dieselnet.com/tech/cat_fund.php, 2000.

[29] W. Addy Majewski. Dieselnet technology guide: Diesel catalysts. http://www.dieselnet.com/tech/cat_scr.php, 2005.

[30] W. Addy Majewski and Hannu E. Jääskeläinen (Eds.). DieselNet Technology Guide: Cellular Monolith Substrates. https://www.dieselnet.com/tech/cat_substrate.php, 1998.

[31] W Addy Majewski and Hannu E. Jääskeläinen (Eds.). Dieselnet technology guide: Catalytic coating & materials. https://www.dieselnet.com/tech/cat_mat.php, 2005.

[32] Nam Chang Mo. NOx reduction by SNCR and it's reaction mechanism under oxidizing diesel flue gas conditions. *Environmental Engineering Research*, 8(1):31–40, 2003.

[33] M J Moore. NOx emission control in gas turbines for combined cycle gas turbine plant. *Proceedings of the Institution of Mechanical Engineers Part a-Journal of Power and Energy*, 211(1):43–52, 1997.

[34] M J Tang, R A Cox, and M Kalberer. Compilation and evaluation of gas phase diffusion coefficients of reactive trace gases in the atmosphere: Volume 1. Inorganic compounds. *Atmospheric Chemistry and Physics*, 14(17):9233–9247, 2014.

[35] M. Tayyeb Javed, Naseem Irfan, and B. M. Gibbs. Control of combustion-generated nitrogen oxides by selective non-catalytic reduction. *Journal of Environmental Management*, 83(3):251–289, 2007.

[36] Michael T. Timko, Scott C. Herndon, Ezra C. Wood, Timothy B. Onasch, Megan J. Northway, John T. Jayne, Manjula R. Canagaratna, Richard C. Miake-Lye, and W. Berk Knighton. Gas Turbine Engine Emissions – Part I: Volatile Organic Compounds and Nitrogen Oxides. *Journal of Engineering for Gas Turbines and Power*, 132(6):061504, 2010.

[37] Enrico Tronconi. Interaction between chemical kinetics and transport phenomena in monolithic catalysts. *Catalysis Today*, 34(3-4):421–427, 1997.

[38] Enrico Tronconi. The role of inter- and intra-phase mass transfer in the SCR-DeNOx reaction over catalysts of different shapes. *Catalysis Today*, 52(2-3):249–258, sep 1999.

[39] Enrico Tronconi and Pio Forzatti. Adequacy of lumped parameter models for SCR reactors with monolith structure. *AIChE Journal*, 38(2):201–210, 1992.

[40] Wiehl, Jürgen and Vogt, Claus Dieter. Ceramic ultra-thin-wall substrates for modern catalysts. *MTZ worldwide*, 64(2):8–11, Feb 2003.

[41] Steve H L Yim, Gideon L Lee, In Hwan Lee, Florian Allroggen, Akshay Ashok, Fabio Caiazzo, Sebastian D Eastham, Robert Malina, and Steven R H Barrett. Global, regional and local health impacts of civil aviation emissions. *Environmental Research Letters*, 10(3):034001, 2015.